Electron Bernstein Wave Heating Experiments on MAST

V. Shevchenko[1], G. Cunningham[1], A. Gurchenko[2], E. Gusakov[2], B. Lloyd[1], M. O'Brien[1], J. Preinhaelter[3], A. Saveliev[2], A. Surkov[2], F.Volpe[1], M. Walsh[1]

[1]EURATOM/UKAEA Fusion Association, Culham, Abingdon, Oxon, OX14 3DB, UK
[2]Ioffe Institute, Politekhnicheskaya 26, 194021 St. Petersburg, Russia
[3]EURATOM/IPP.CR Association, Institute of Plasma Physics, 18221 Prague, Czech Republic

e-mail: vladimir.shevchenko@ukaea.org.uk

Abstract. Burning plasma spherical tokamak (ST) designs rely on off-axis current drive and non-solenoid start-up techniques. Electron Bernstein waves (EBW) may provide efficient off-axis heating and current drive (CD) in high density ST plasmas. EBW may also be used in the plasma start-up phase due to the fact that EBW absorption and CD efficiency remain high even in relatively cold plasmas. EBW studies on the Mega Amp Spherical Tokamak (MAST) can be subdivided into four separate subjects: thermal EC emission observations from overdense plasmas; EBW modeling; proof-of-principle EBW heating experiments with the existing 60 GHz gyrotrons; EBW assisted plasma start-up at 28 GHz. These studies are also aimed at determining the potential for a high power EBW system for heating and CD on MAST; the optimum choices for the frequency and launch configuration of such as system are key issues. A major advance in the integrated modelling of EBW, involving a suite of codes, has been achieved. The EBW excitation in the plasma is first considered as a full wave 1D mode-coupling problem in slab geometry. Then propagation of the EBW is computed using an EBW ray-tracing code, which implements the fully electromagnetic, hot plasma dispersion function. The ray tracing data are then used in the BANDIT code in a self-consistent, relativistic 3D Fokker-Planck treatment to calculate the heating and driven current profiles. The modelling shows that the operating frequency for efficient EBW heating and CD on MAST should be in the range of the fundamental EC resonance or its lower harmonics, with the best frequency choice for the high power RF source in the range 16–30 GHz. Proof-of-principle EBW heating experiments have been conducted on MAST using the existing 60 GHz, 1 MW complex. EBW heating effects have clearly been observed for the first time in an ST. A 28 GHz EBW start-up system (200 kW, 40 ms) is being commissioned, and according to our modelling should generate plasma current up to ~100 kA during the plasma start-up phase giving the prospect of a fully non-inductive plasma start-up scenario.

1. Introduction

One of the main objectives of the Mega Amp Spherical Tokamak (MAST) programme is to explore the potential of the spherical tokamak (ST) concept as a basis of a fusion Component Test Facility and a high beta fusion power plant [1]. Burning plasma STs rely on off-axis current drive and start-up techniques which do not require a central solenoid. Electron Bernstein Waves (EBW) may provide efficient off-axis heating and current drive (CD) in high density ST plasmas. Following successful demonstration of EBW current drive at Culham in the COMPASS-D tokamak, by exploiting extraordinary-Bernstein (X-B) mode conversion with the X-mode launched from the high field side (HFS) [2], with efficiency $\eta_{20} = n_{e20} I_{rf} R P_{rf}^{-1} \sim 0.035$ $AW^{-1}m^{-2}$ exceeding that achievable with conventional ECRH for similar plasma parameters, EBW heating experiments have continued on MAST using the existing 60 GHz gyrotrons.

EBWs are a promising means of plasma heating and current drive in STs. Extensive ray tracing modelling and thermal EBW emission (16 - 67 GHz) measurements suggest the preferable operating frequency for efficient EBW heating and CD must be in the range of the fundamental EC resonance or its lower harmonics [3, 4]. For MAST, this requires a high power RF source in the range of 16 – 30 GHz, and so an EBW CD system in this range is presently under consideration for future implementation on MAST. A 60 GHz (~1 MW) gyrotron complex is already available. It is equipped with a steerable 7 beam launching system. Despite the fact that the operating frequency is far from optimum a number of physical processes can be studied with the existing experimental set-up.

2. EBW Modelling

The optimum choice of frequency and launch configuration for EBW heating and CD is a key issue for future applications in MAST. The propagation and dispersion of EBWs is a complicated function of electron temperature, density and magnetic field in the plasma. Magnetic field topology in STs is characterised by relatively large variations of poloidal and toroidal components over the major radius, and by comparable poloidal and toroidal fields near the plasma edge. This fact makes the task of EBW heating and CD optimisation multi-parametric. Modelling was conducted in a parametric space including variations of heating frequency over the fundamental and higher harmonics, different launch polarisation and vertical position of the launcher. The goal was to find the optimal parameters for off-axis CD and for central heating and CD. A major advance in the integrated modelling of EBW, involving a suite of codes, has been achieved.

A Gaussian beam incident upon the plasma is first Fourier decomposed in plane waves of various k-vectors and propagation of each Fourier component in vacuum and plasma (inside and outside separatrix) is then considered separately. The EBW excitation in the plasma is then treated as a full wave 1D mode-coupling problem in slab geometry as described in [5]. Calculations are performed in Cartesian co-ordinates with the x-axis perpendicular to the plasma boundary and with the origin located at the point where the beam centre crosses the plasma surface. According to this approach the EBW is excited in the vicinity of the Upper Hybrid Resonance (UHR) where the cold plasma approximation for the electromagnetic mode is violated. To describe the mode conversion it is sufficient to find a solution of the cold plasma wave equation vanishing in the high-density evanescent region and matching to the incident and reflected waves at the plasma edge. The UHR is a singular point of the wave equation. In the immediate vicinity of this point the solution can be presented analytically and the theory gives a rule for choosing its proper branch. The singularity of the x-component of the electric field is a pole and its residue determines the complex Wentzel-Kramers-Brillouin (WKB) amplitude of the outgoing EBW. This approach does not require applicability of the WKB approximation for the electromagnetic mode and includes both the O-X-B mode conversion and the direct X-B tunnelling. The coupling code solves the cold plasma wave equation for each Fourier component of the antenna beam using a Runge-Kutta method and finds the required residue. The EBW electric field distribution for the whole beam is then computed at the flux surface close to the UHR with the use of the inverse Fourier transformation. The electric field distribution serves as the starting condition for the EBW beam in a ray-tracing code. Thus, the initial conditions for EBW rays are prescribed unambiguously for the specified launch parameters, including the beam width, divergence, polarization and the antenna position.

Propagation of the EBW is then computed using the EBW ray-tracing code, which can use either a relativistic electrostatic or a non-relativistic fully electromagnetic hot plasma dispersion function. This code calculates EBW absorption along the rays using a relativistic electrostatic approximation [6] and can be used for the preliminary, scoping stage of the RF launch optimisation to obtain a required localisation of the RF power deposition by variation of the antenna position, RF frequency or plasma parameters. For more detailed calculations including current drive, the ray tracing data are then used in the BANDIT code [7] in a self-consistent, relativistic 3D Fokker-Planck treatment to calculate the heating and driven current profiles. Both ray tracing and Fokker-Planck codes use the full tokamak equilibrium. While the relativistic terms are used throughout in the damping calculations, the fully relativistic electrostatic dispersion relation is only used in the EBW ray propagation calculations at the final stage of heating and CD simulations because it typically requires 20 times longer run

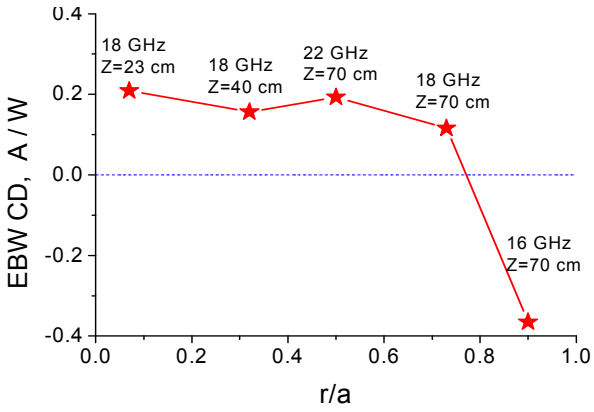

FIG. 1. Predicted EBW CD efficiency over minor radius in MAST with 1 MW injected power for indicated frequencies and vertical positions of the launcher. Relativistic effects included.

time in comparison with non-relativistic ray-tracing. Here we summarise the potential of EBW CD on MAST based on our modelling results.

The main objective for the EBW CD system is to provide efficient off-axis current drive radially localised at r/a ~ 0.7. The central current in steady-state scenarios is supposed to be sustained by neutral beam injection. Fig. 1 illustrates EBW CD capabilities over the minor radius. The target plasma used in our modelling has a major radius of 0.83 m, elongation of 2.5, aspect ratio of 1.43, plasma current of 1 MA, toroidal field (magnetic axis) of 0.52 T, a flat density profile with $n_{e0} = 4.5 \cdot 10^{19}$ m^{-3} and a parabolic electron temperature profile with $T_{e0} = 4$ keV. It was assumed that the vertical position z of the launcher can be chosen and the RF frequency can be varied within the range of fundamental resonance. Obviously, the toroidal field can be varied instead of RF frequency assuming the other parameters unchanged. As seen in Fig. 1 the CD efficiency remains almost constant at ~0.2 A/W over the radii r/a from 0 to ~0.75. Then it crosses 0 at r/a ≈ 0.8 and becomes negative in the peripheral region, where Ohkawa current dominates over Fisch-Boozer current. Thus, for the NBI CD assist the optimal frequency is about 18.5 GHz with the launcher positioned at about 75 cm above/below the midplane for co-/counter- CD. However, if broader applications are considered for EBW CD on MAST, such as a fully non-inductive plasma formation, localised current density control over the radius etc., a few switchable launchers must be employed allowing central and mid-radius CD. The modelling suggests the preferable operating frequency for efficient EBW heating and CD must be in the range of the fundamental EC resonance or its lower harmonics [3]. An EBW CD system at the fundamental resonance is presently under consideration for future implementation on MAST.

3. Proof-of-Principle EBW Heating Experiments

The experiments were conducted at 60 GHz with injected RF power up to 0.8 MW. The first stage of the O-X-B mode conversion process occurs in the $\omega_{RF} = \omega_{pe}$ layer and it requires the O mode to be launched within a narrow range of angles, so called a mode conversion "window", with respect to the edge magnetic field. The angular width of this "window" depends mainly on the local density gradient length-scale. Thus, high density plasma with a steep density gradient at $n_e = 4.5 \cdot 10^{19}$m^{-3} is needed for the 60 GHz experiments. This constraint requires plasmas close to the limit of MAST operational space. Therefore three different plasma scenarios have been developed especially for these experiments (see Fig. 2).

3.1. The first scenario (Fig. 2a) is based on the high density ELM-free H-mode. It offers a relatively broad (±5°) O-X-B mode conversion window due to a high density gradient in the conversion zone but EBW absorption, as predicted by modeling, is expected to be very peripheral (r/a ~ 0.9). As the O-X-B mode conversion occurs in relatively cold plasma layers close to the separatrix, non-linear phenomena were anticipated in this scenario [8, 9]. The electric field of the wave approaching the UHR increases dramatically and at some level can cause non-linear effects, in particular parametric decay instability. Parametric decay can lead to redistribution of the incident power between plasma species and cause partial reflection of the injected power especially when excited at the plasma edge.

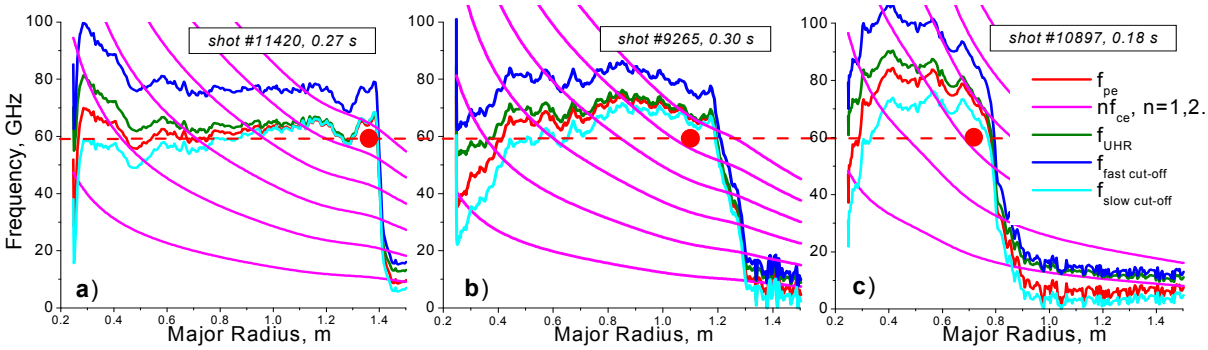

FIG. 2. Plasma scenarios developed for EBWH experiments. Midplane resonances and cut-offs illustrate RF accessibility to the bulk plasma. Power deposition is indicated by red spots: ***a)*** *ELM-free H-mode,* ***b)*** *sawtoothing H-mode,* ***c)*** *Ohmic H-mode.*

RF power is expected to be deposited at high EC harmonics (between $5\omega_{ce}$ and $6\omega_{ce}$) leading to peripheral absorption and ineffective heating in this scenario. Nevertheless, there was clear evidence of the mode conversion process as parametric decay waves originating from the UHR were observed using a specially designed lower hybrid (LH) probe. Fig. 3a illustrates a strong plasma emission enhancement around 134 MHz during the RF pulse when the plasma reached the overdense state.

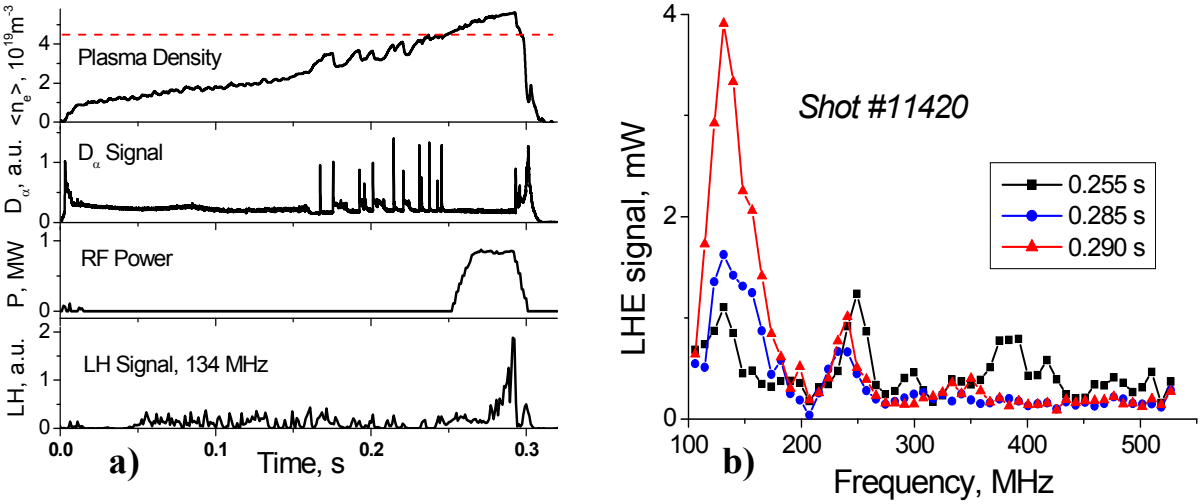

FIG. 3. ***a)*** *Line averaged plasma density, D_α signal and RF power in 60 GHz EBW heating experiment with ELM-free H-mode. The plasma becomes overdense i.e. the mode conversion becomes possible when plasma density is above the red dashed line. Note the strongly increased LH signal peaked at 134 MHz during RF pulse when plasma reached the overdense state. The probe position is about 5 cm outside the last closed flux surface.* ***b)*** *LH emission spectra during RF pulse.*

The enhanced emission is very localised in frequency (Fig. 3b). The half width of the spectral peak is about 10 MHz. Due to the fact that the spectral maximum is close to the LH resonance frequency in the UHR region for 60 GHz we identify this radiation as generated by the parametric decay instability occurring in the UHR.

A theoretical study of parametric decay of the incident upper hybrid (UH) wave into another UH wave plus LH wave has been conducted in collaboration with the Ioffe Institute. The power threshold and growth rates of the absolute decay instability were evaluated for the specific conditions of low magnetic field typical for the ST. According to [10] the threshold for the fundamental mode of the parametric decay can be estimated from the expression:

$$\frac{P^*_{UHR}}{\pi\rho^2}\left[\frac{W}{cm^2}\right] = 2\cdot 10^{-3}\,\frac{f^{1/3}T_{eff}^{11/12}T_e^{5/4}B^{1/3}}{L^{4/3}}\left[\frac{W}{cm^{2/3}T^{1/3}GHz^{1/3}eV^{13/6}}\right] \qquad (1)$$

where $T_{eff} = T_e + 4T_i$, ρ is the e^{-1} (electric field) radius of the heating beam spot and L is the inhomogeneity scale: $L^{-1} = \text{grad}(n_e)/n_e + 2\omega_{ce}^2/\omega_{pe}^2 \text{grad}(B)/B$. All plasma parameters are taken at the UHR. For typical MAST parameters at f = 60 GHz, $T_i \approx T_e$ = 140eV, B =*0.38* T, L = 3 cm, the parametric decay (1) can arise at $P^*_{UHR}/(\pi\rho^2) \approx 260$ W/cm^2, i.e. if the pump power exceeds $P^*_{UHR} \approx 80$ kW in any beam spot of $\rho \approx 10$ cm radius. The obtained value allows us to estimate the coupling to EBW to be no less than 50% in at least one of the beams, because beam overlapping is negligible.

3.2. The second scenario (Fig. 2b) is based on a sawtoothing H-mode plasma, in which a high density gradient zone allowing the O-X-B conversion appears deeper into the plasma. In this scenario the density gradient scale length is very short for pedestal densities up to $2\cdot10^{19}$m^{-3} and has a relatively moderate value at higher densities. This allows us to shift the plasma cut-off (O-X conversion layer) by 10-15 cm deeper into the plasma, avoiding interception by the upper EC harmonic. As a result the mode conversion window is narrower ($\pm3^o$) in this case but the EBW power deposition can reach as far in as r/a ~ 0.6.

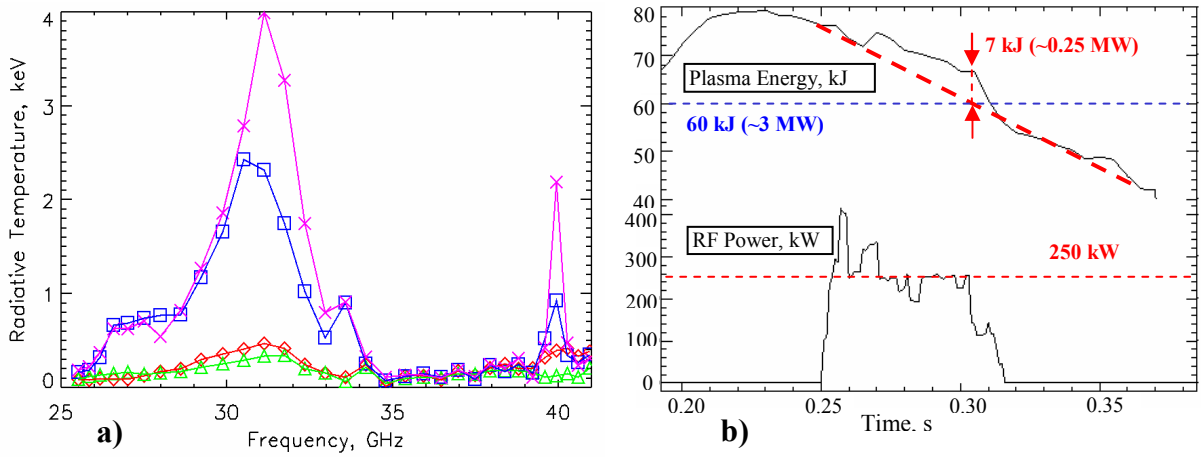

FIG. 4. ***a)*** *EBW radiative temperature profiles measured from 2ω_{ce} during ELM-free periods at optimum toroidal field: 0.2 s – red, 0.23 s – green, 0.26 s – blue, 0.28 s – magenta. RF power was injected from 0.25 s to 0.31 s. Note radiative temperature enhancement during RF injection. Narrow peak at 40 GHz is due to 60 GHz stray radiation.* ***b)*** *EBW heating results. Both (a) and (b) are for sawtoothing H-mode plasmas.*

A toroidal field (TF) scan has been conducted within the range of 60 GHz O-mode cut-off intersections with the 5ω_{ce} and 6ω_{ce} harmonics. The aim was to enhance the EBW emission from the lower EC harmonics during RF injection. The TF scan has shown that the EBW emission enhancement (see Fig. 4a) during RF injection has a well-pronounced maximum when the O-mode cut-off is located at about 2/3 of the distance between the 5ω_{ce} and 6ω_{ce} harmonics. This scenario with optimised TF has provided some evidence of plasma heating during RF power injection. The O-X-B mode conversion and consequently heating is strongly modulated by sawteeth and ELMs, hence, the effect is better seen after averaging over 3 shots. Fig. 4b indicates a ~10% increase of the total plasma energy (EFIT) during the RF pulse with an average injected RF power of ~0.25 MW. The total heating power (NBI + Ohmic) in these shots was about 3 MW. It should be noted that no parametric decay has been observed in sawtoothing H-mode. This can be explained by the fact that the X-B mode conversion occurs in the deeper plasma layers where the electron temperature is higher in sawtoothing H-mode ($T_e^{UHR} \approx$ 350 eV, shot #9265 at 0.3 sec) than in ELM-free H-mode ($T_e^{UHR} \approx$ 150 eV, shot #11420 at 0.27 sec). Equation (1) gives an approximately quadratic dependence on temperature so the power threshold was not exceeded in this scenario.

3.3. In the third scenario, high density ohmic H-mode (Fig. 2c) is achieved by plasma compression in major radius. Because plasma is compressed into a higher magnetic field, r/a ~ 0.4 becomes accessible transiently at $3\omega_{ce}$ and then at $2\omega_{ce}$ during the compression process.

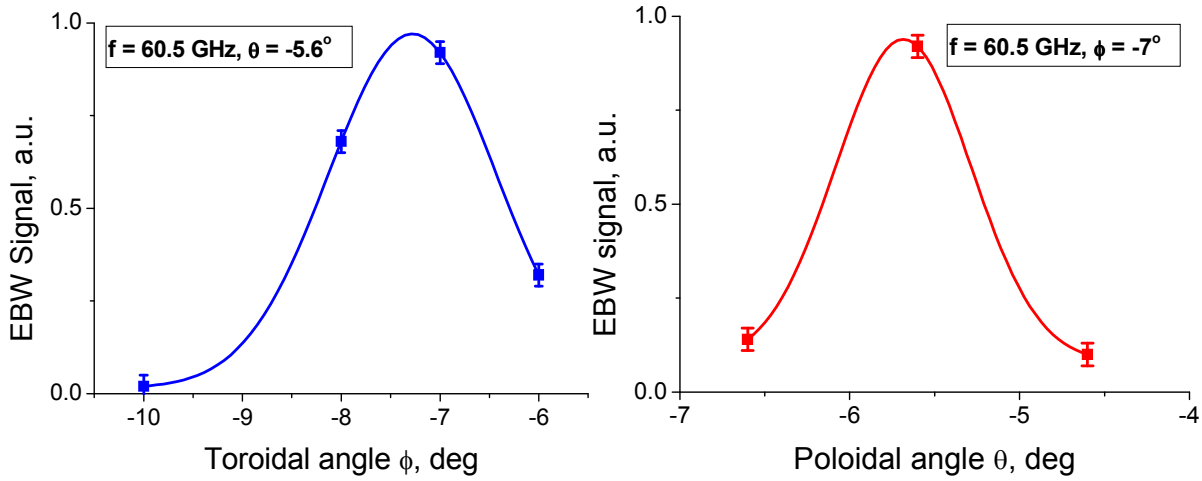

FIG. 5. Launch angle optimization for injection into Ohmic H-mode plasma using EBW emission measurements at 60.5 GHz through the launching antenna.

The mode conversion window (±1.5°) is very restrictive in this case hence the thermal EBW plasma emission was used for the launch optimization (Fig. 5).

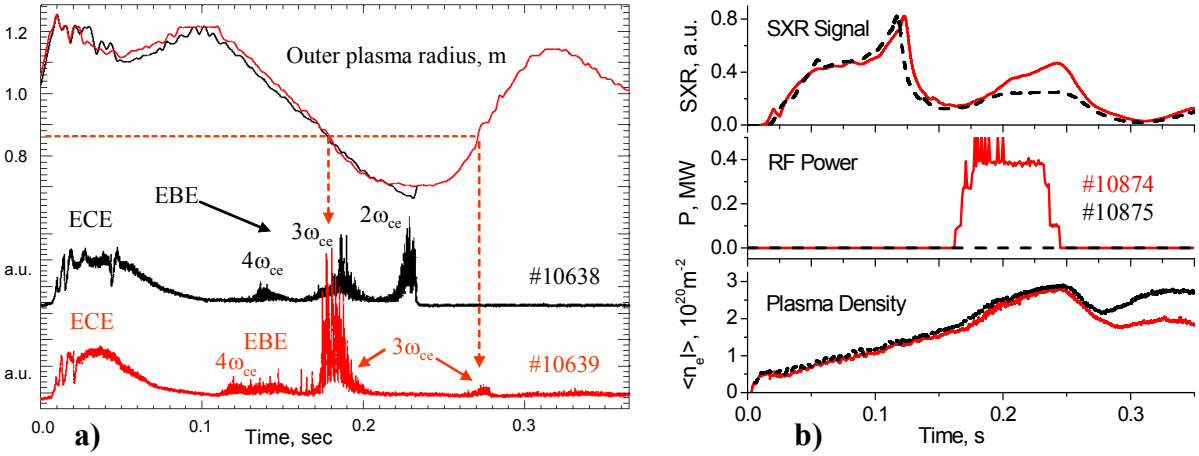

*FIG. 6. **a)** EBW emission (60.5 GHz) in high density Ohmic H-mode during plasma compression. As the plasma boundary moves into the higher magnetic field during compression, EBW emission comes first from $4\omega_{ce}$, then from $3\omega_{ce}$ and finally from $2\omega_{ce}$. The $2\omega_{ce}$ emission is seen when the outer radius is smaller than 0.7 m (shot #10638). **b)** SXR signal, RF power and line integrated plasma density in RF heated shot (red solid line) and ohmic shot (black dashed line). Note a strong increase of SXR signal during RF injection.*

EBW emission measurements at 60.5 GHz show two distinctive maxima in time intervals 0.17 – 0.2 s and 0.22 – 0.25 s corresponding to accessibility windows for $3\omega_{ce}$ and then $2\omega_{ce}$ (Fig. 6a). Thus the RF pulse timing was chosen to cover both time intervals. The SXR signal was practically doubled during the RF pulse in comparison with the ohmic plasma as illustrated on Fig. 6b. During the intervals when $3\omega_{ce}$ and $2\omega_{ce}$ become accessible the SXR signal shows a higher rate of increase. Thomson scattering measurements at 0.18 s and 0.2 s show about a 10% increase in electron temperature in the RF heated shots in comparison to the ohmic shots (Fig. 7). Unfortunately, it is not possible to use the LH probe in this scenario because the plasma boundary was moving during the shot.

4. 28 GHz start-up System

It has been shown experimentally that EBW CD excited with the X-mode launched from the HFS is capable of producing a substantial amount of current [2], which could possibly sustain plasma stability during plasma current flat top. A non-inductive plasma current start-up scenario based on EBW CD at 28 GHz has been proposed for MAST [11]. This scheme assumes that low-density plasma will be produced by RF pre-ionisation around the fundamental electron cyclotron resonance layer. Then a double mode conversion scheme is considered for EBW excitation in plasmas with densities lower than the O-mode cut-off density (see Fig. 8). The scheme consists of the conversion of the O-mode, incident from the low field side of the tokamak, into the X-mode with the help of a grooved mirror-polariser incorporated in a graphite tile on the central rod. The X-mode reflected from the polariser propagates back to the plasma and experiences a subsequent X-EBW mode conversion near the upper hybrid resonance. Finally the excited EBW mode is totally absorbed before it reaches the EC resonance, due to the Doppler shift. The absorption of EBW remains high even in cold plasma. Furthermore, EBW can generate significant plasma current during the plasma start-up phase giving the prospect of a fully non-inductive plasma start-up scenario.

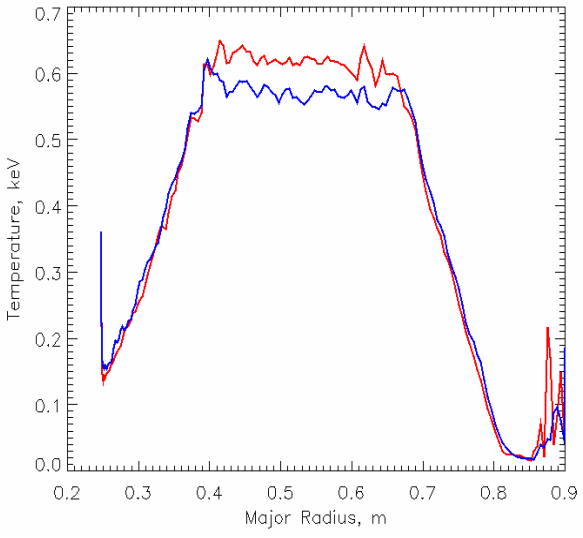

FIG. 7. Electron temperature profiles measured by Thomson scattering in RF heated (red) and ohmic (blue) plasmas at 0.18 s.

These separate stages have each been demonstrated on a number of tokamaks [2, 12-14]. The proposed scenario combines their advantages in order to achieve a substantial (~100 kA) non-inductive plasma current in MAST. The plasma obtained with the proposed start-up scenario is restricted to low densities ($n_{e0} < 10^{19}m^{-3}$ for 28 GHz) to allow O-mode propagation to the mirror-polariser. As soon as the start-up phase is completed the plasma current, in principle, can be sustained further by EBW CD based on O-X-B conversion of the lower frequency wave launched from the LFS.

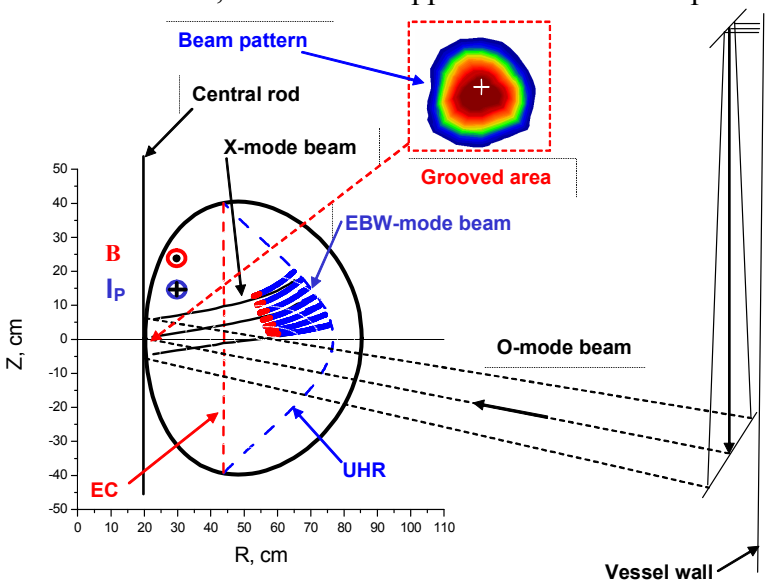

FIG. 8. Schematic (poloidal view) of the EBW CD plasma initiation. EBW ray-tracing simulations were performed with experimental data. The equilibrium was taken from a solenoid start-up scenario at 30 ms, shot #9867 in MAST and is before the plasma reaches its final size and shape. The RF beam pattern, as measured at low power, is well within the grooved area of the graphite mirror-polariser.

The 28 GHz start-up system has been designed and is now being commissioned on MAST. The gyrotron is capable of delivering up to 200 kW for 40 ms. Low-power tests have been conducted using a full scale mock-up assembly of the launcher before installation on MAST. The RF beam pattern measured at the graphite tile shows that the beam is very close to Gaussian and 98% of the power is well within the grooved area of the mirror-polariser as illustrated in Fig. 8.

5. Conclusions

A dedicated complex of high power RF heating systems, EBW diagnostics, and modeling tools has been developed at Culham in order assess the potential of EBW assisted plasma start-up, EBW heating and CD in MAST. A major advance in the integrated modelling of EBW, involving a suite of codes, has been achieved, allowing us to address the optimum frequency and launch configuration for a future MAST EBW heating and CD system and to study EBW assisted start-up.

Proof-of-principle EBW heating experiments have been conducted on MAST using 3 special plasma scenarios. It was shown that the O-X-B mode coupling efficiency was at least 50 % in high density ELM-free H-mode plasmas. In sawtoothing H-mode plasmas a 10% increase of plasma energy was measured during RF injection. In small ohmic H-mode plasmas the enhanced SXR emission and about 10% increase of electron temperature were measured. EBW heating has therefore clearly been observed in MAST via the O-X-B mode conversion process.

6. Acknowledgments

This work was funded jointly by the United Kingdom Engineering and Physical Sciences Research Council and by the European Communities under the contract of association between EURATOM and UKAEA. The views and opinions expressed in this paper do not necessarily reflect those of the European Commission.

7. References

1. B. LLOYD, overview paper OV/2-3 at this conference
2. V. SHEVCHENKO *et al*., Phys. Rev. Lett. **89**, 265005 (2002)
3. V. SHEVCHENKO *et al*., in Proc. 13th Joint Workshop on ECE and ECRH, Nizhny Novgorod, Russia, p. 162, (2004)
4. G. TAYLOR *et al.,* Physics of Plasmas, **11**, No 10, p. 4733 (2004)
5. A. P. PILIYA, E. N. TREGUBOVA, Plasma Phys. Control. Fusion **47,** 143 (2005)
6. A. N. SAVELIEV, Plasma Phys. Control. Fusion, **47**, 2003, (2005)
7. M. O'BRIEN *et al*., in Proc. IAEA TCM on Advances in Simulation and Modelling of Thermonuclear Plasmas, Montreal, (IAEA, Vienna, 1993) p.527.
8. F.C. MCDERMOTT *et al*., Phys. Fluids, **25**, No 9, p. 1488 (1982)
9. H.P. LAQUA *et al*., Phys. Rev. Lett. **78**, 18, 3467 (1997)
10. A. SURKOV *et al*., in Proc. 32nd EPS Conference on Plasma Physics and Controlled Fusion, Tarragona, Spain, ECA vol. 29C, P-5.103 (2005)
11. V. SHEVCHENKO *et al*., in Proc. 13th Joint Workshop on ECE and ECRH, Nizhny Novgorod, Russia, p. 255, (2004)
12. T. MAEKAWA *et al*., Phys. Rev. Lett. **86**, 3783 (2001)
13. M. GRYAZNEVICH *et al*., Nucl. Fusion, **46**, S573 (2006)
14. C.B. FOREST *et al*., Phys. Plasmas, **1**(5), 1568 (1994)